Liquid phase epitaxy growth of $Pb_{1-x}Sn_xSe_{1-y}Te_y$ alloys lattice matched with BaF_2

Patrick J. McCann and Dongfan Zhong
School of Electrical Engineering, University of Oklahoma, Norman, Oklahoma 73019

(Received 26 July 1993; accepted for publication 4 October 1993)

IV–VI semiconductor quaternary alloys lattice matched with BaF_2 substrates have been grown by liquid phase epitaxy. X-ray diffraction analysis shows that liquid $(Pb_{1-x_L}Sn_{x_L})_{0.99}(Se_{1-y_L}Te_{y_L})_{0.01}$ solutions produce $Pb_{1-x_S}Sn_{x_S}Se_{1-y_S}Te_{y_S}$ alloys lattice matched with the substrate when $y_L=60\%$, 58%, and 57%, and $x_L=20\%$, 40%, and 60%, respectively. These data, which can be used to fabricate lattice-matched heterostructure optoelectronic devices covering the 6–30 μm spectral range, show that smaller tellurium concentrations in the liquid growth solution yield lattice-matched alloys as the tin content increases. This is despite the fact that the tellurium content in the isoperiodic solid solution alloy increases with tin content. This result suggests that the chemical potential of tellurium in $Pb_{1-x_S}Sn_{x_S}Se_{1-y_S}Te_{y_S}$ solid solutions decreases as tin and tellurium concentrations increase. It is argued that this highly nonideal behavior is due to the decreasing strain energy driven segregation of tellurium from the solid to the liquid as the tin concentration increases.

I. INTRODUCTION

The fabrication of reliable far-infrared optoelectronic heterostructure devices requires development of suitable narrow gap semiconductors in which the band gap and lattice parameter can be independently controlled. A materials system satisfying these requirements is the quaternary IV–VI semiconductor, $Pb_{1-x_S}Sn_{x_S}Se_{1-y_S}Te_{y_S}$. This solid solution pseudobinary alloy can be used as the active region in either detectors or lasers designed to operate in the 6–30 μm spectral range. Lattice-matched $Pb_{1-x_S}Sn_{x_S}Se_{1-y_S}Te_{y_S}$ quaternary layers have been grown on $Pb_{0.80}Sn_{0.20}Te$ and PbSe substrates, and double heterostructure lasers fabricated from these materials have been demonstrated.[1,2] Further device development, however, has been hindered by the limited availability, small size, and high cost of these IV–VI semiconductor substrates.

Lattice-matched growth of $Pb_{1-x_S}Sn_{x_S}Se_{1-y_S}Te_{y_S}$ on a more readily available substrate material would greatly facilitate far-infrared device development. A promising substrate material for such epitaxy is BaF_2. High quality, epitaxial-grade BaF_2 is commercially available in large sizes and is relatively inexpensive. Its lattice parameter is between that of PbSe and PbTe, and its crystal structure is similar to the IV–VI semiconductors (barium cations occupy the same face-centered-cubic sublattice positions that group IV and group VI elements occupy in the IV–VI semiconductors). Furthermore, the thermal expansion coefficient of BaF_2 is nearly the same as that of the IV–VI semiconductors. For these reasons, BaF_2 substrates have been used for IV–VI semiconductor vapor phase epitaxy since 1970.[3]

In addition to growth on bulk BaF_2, IV–VI semiconductors have been grown on BaF_2-coated silicon substrates.[4] Such growth has enabled integration of IV–VI semiconductor infrared detector arrays with silicon circuitry.[5] Although various compositions of IV–VI semiconductor alloys have been grown on both bulk BaF_2 and BaF_2-coated silicon substrates, there are no reports of lattice-matched quaternary alloy growth on BaF_2. In our work, we are interested in fabricating far-infrared heterostructure devices using a new liquid phase epitaxy (LPE) process that has recently been used to grow $PbSe_{0.78}Te_{0.22}$ layers lattice matched with (100) BaF_2 substrates.[6] Growth of smaller band gap $Pb_{1-x_S}Sn_{x_S}Se_{1-y_S}Te_{y_S}$ quaternary layers will enable, for example, fabrication of double heterostructure (DH) lasers. Accordingly, this article reports on the LPE growth and characterization of $Pb_{1-x_S}Sn_{x_S}Se_{1-y_S}Te_{y_S}$ quaternary alloys lattice matched with BaF_2 substrates.

II. $Pb_{1-x_S}Sn_{x_S}Se_{1-y_S}Te_{y_S}$ QUATERNARY ALLOYS

Employing a generalized version of Vegard's law,[7] the lattice parameter of $Pb_{1-x_S}Sn_{x_S}Se_{1-y_S}Te_{y_S}$ quaternary alloys can be expressed as

$$a=6.126+0.334y_S-0.123x_S-0.009x_Sy_S. \quad (1)$$

The condition for lattice matching the 6.200 Å lattice parameter of BaF_2 is therefore

$$y_S=\frac{0.074+0.123x_S}{0.334-0.009x_S}. \quad (2)$$

The band gap of quaternary $Pb_{1-x_S}Sn_{x_S}Se_{1-y_S}Te_{y_S}$ at 77 K can be expressed as[8]

$$E_g=0.175-0.895x_S+0.044y_S+0.36x_Sy_S. \quad (3)$$

In addition to composition dependence, the band gaps of $Pb_{1-x_S}Sn_{x_S}Se_{1-y_S}Te_{y_S}$ alloys are also very sensitive to temperature variations. IV–VI semiconductor lasers, therefore, have extremely wide temperature tuning ranges. For example, varying the heat sink temperature of a $PbTe/Pb_{0.782}Sn_{0.218}Te/PbTe$ DH laser from 12 to 114 K varied the emission wavelength from 15.9 to 8.54 μm.[9]

 0021-8979/94/75(2)/1145/6/$6.00

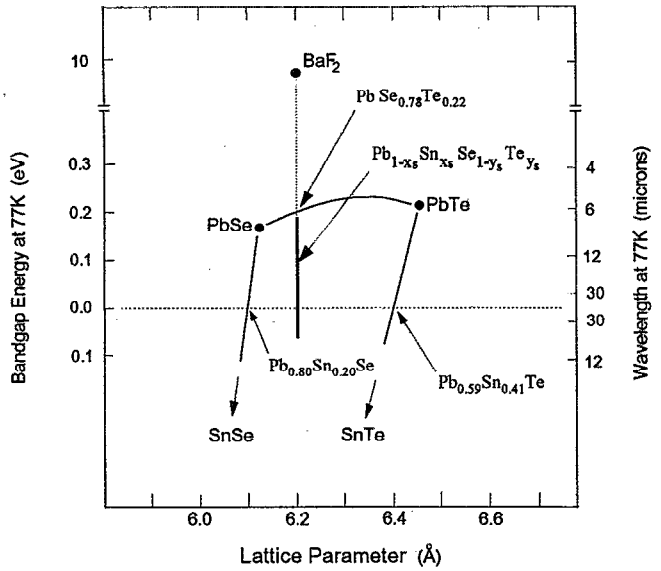

FIG. 1. Band gaps and corresponding cutoff wavelengths at 77 K plotted as a function of lattice parameter for various IV–VI semiconductors and BaF_2.

This property makes IV–VI semiconductor lasers useful for high resolution infrared spectroscopy applications.

IV–VI semiconductor alloys exhibit a distinctive band crossover phenomenon. As the tin content increases, the band gap decreases until, at a certain composition, the band gap becomes zero. Beyond this point, the band gap begins to increase with tin content, and the temperature coefficient changes sign, i.e., instead of increasing, the band gap decreases with increasing temperature. This behavior has been observed in both $Pb_{1-x_S}Sn_{x_S}Se$ (Ref. 10) and $Pb_{1-x_S}Sn_{x_S}Te$ (Ref. 11) ternary alloys and is attributed to band inversion at the L point in the Brillioun zone. We expect similar behavior in quaternary $Pb_{1-x_S}Sn_{x_S}Se_{1-y_S}Te_{y_S}$ alloys lattice matched with BaF_2 substrates where the band gap at 77 K can be approximated by substituting Eq. (2) into Eq. (3):

$$E_g \approx 0.185 - 0.799x_S + 0.133x_S^2. \quad (4)$$

Negative band gap values for $x_S > 24\%$ represent an inverted band structure. Figure 1 is a band gap versus lattice parameter plot for $Pb_{1-x_S}Sn_{x_S}Se_{1-y_S}Te_{y_S}$ alloys and BaF_2. The quaternary alloy lattice matched with BaF_2 is indicated.

PbSe, PbTe, and SnTe all have NaCl-type crystal structures, but SnSe has an orthorhombic crystal structure. SnSe-rich compositions of $Pb_{1-x_S}Sn_{x_S}Se_{1-y_S}Te_{y_S}$ solid solutions will, therefore, exhibit a two-phase microstructure due to the immiscibility of SnSe in PbTe. The solid solubility limit of SnSe in PbSe has been reported to be 43 mole % SnSe,[12] while for alloys lattice matched with BaF_2 the two-phase region begins at a tin concentration of approximately 68%.[13] This limit on the composition of $Pb_{1-x_S}Sn_{x_S}Se_{1-y_S}Te_{y_S}$ solid solutions lattice matched with BaF_2 nevertheless still allows a wide range of band gaps from 185 meV, through zero, to negative 300 meV at 77 K.

The first reported growth of quaternary $Pb_{1-x_S}Sn_{x_S}Se_{1-y_S}Te_{y_S}$ alloys was accomplished by melting stoichiometric quantities of the elements.[14] In one series of experiments, $Pb_{1-b}Sn_bSe_{1-b}Te_b$ alloys were prepared by mixing $(1-b)$ moles of PbSe and b moles of SnTe. Coincidentally, an alloy with the composition $Pb_{0.70}Sn_{0.30}Se_{0.70}Te_{0.30}$ had a measured lattice parameter of 6.195 Å, very close to that of BaF_2. Optical absorption studies were also performed, but only on alloys with SnTe concentrations up to 6%. The reported data do show that at 82 K the band gap decreases from 180 meV for PbSe to 160 meV for $Pb_{0.94}Sn_{0.06}Se_{0.94}Te_{0.06}$.

Historically, liquid phase epitaxy has been the primary growth technique for initial materials studies leading to the development of new heterostructure optoelectronic devices. This is due to the fact that LPE is an economical method for producing high quality material. LPE growth of $Pb_{1-x_S}Sn_{x_S}Se_{1-y_S}Te_{y_S}$ quaternary alloys having compositions that are lattice matched with BaF_2, however, will require knowledge of the relevant portion of the liquid-solid Pb-Sn-Se-Te phase diagram. Such data exist for growth of quaternary alloys lattice matched with $Pb_{0.80}Sn_{0.20}Te$ (Ref. 1) and PbSe (Ref. 2) substrates, and data exist for growth of ternary $PbSe_{0.78}Te_{0.22}$ layers lattice matched with BaF_2 substrates.[6] In the latter case, for example, liquid solutions of $Pb_{1-z}(Se_{0.40}Te_{0.60})_z$ produce the desired lattice-matched alloy. In general, we would like to know what liquid solution compositions, $(Pb_{1-x_L}Sn_{x_L})_{1-z}(Se_{1-y_L}Te_{y_L})_z$ produce solid $Pb_{1-x_S}Sn_{x_S}Se_{1-y_S}Te_{y_S}$ quaternary alloys that are lattice matched with BaF_2.

III. EXPERIMENTAL PROCEDURE

A standard sliding-substrate LPE graphite boat under a flowing hydrogen ambient was used to grow $Pb_{1-x_S}Sn_{x_S}Se_{1-y_S}Te_{y_S}$ quaternary alloys. Lead, tin, and polycrystalline pieces of the binaries PbTe and PbSe were weighed to yield various compositions of $(Pb_{1-x_L}Sn_{x_L})_{1-z}(Se_{1-y_L}Te_{y_L})_z$ liquid solutions. The chalcogen content z was fixed at 1% which resulted in liquidus temperatures of around 530 °C. The liquidus temperature, which dictates the LPE growth initiation temperature, was measured by observing the surface of a slowly heated undercooled liquid growth solution and noting the temperature at which the last piece of solid dissolves. Our measured values are consistent with previously published data[2] that show that $(Pb_{1-x_L}Sn_{x_L})_{1-z}(Se_{1-y_L}Te_{y_L})_z$ liquidus temperatures increase with z. Cleaved (111)-oriented BaF_2 substrates were used for all growths. Growth was initiated 2° below the liquidus temperature by positioning the BaF_2 substrate under the growth solution. This growth proceeded for 10 min while the furnace cooled at 2° per minute. Growth was terminated by pulling the substrate out from under the growth solution.

Optical and scanning electron microscopic analyses,

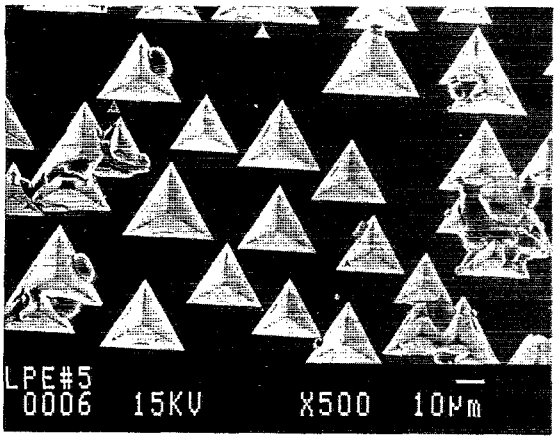

FIG. 2. SEM showing {100}-faceted $Pb_{1-x_S}Sn_{x_S}Se_{1-y_S}Te_{y_S}$ crystallites grown by LPE on a (111) BaF_2 substrate. LPE growth was initiated at 530 °C from a $(Pb_{0.60}Sn_{0.40})_{0.99}(Se_{0.80}Te_{0.20})_{0.01}$ liquid solution and proceeded for 10 min of cooling at 2° per min.

see Fig. 2, of the grown material showed a trigonal pyramid crystallite morphology. This type of growth morphology has also been observed for PbSe growth on (111) BaF_2 at similar growth initiation temperatures.[15] In both cases, the IV–VI semiconductor crystallites were oriented with the BaF_2 substrate. It is believed that this crystallite morphology is due to an incomplete epitaxy-enabling substrate surface reaction[16] in which selenium and tellurium react with the BaF_2 substrate forming a Ba(Se,Te) reaction product that catalyzes IV–VI semiconductor nucleation.[17] Growth at higher temperatures, above 610 °C, where the reaction product completely covers the BaF_2 surface, has resulted in continuous PbSe (Ref. 15) and lattice-matched $PbSe_{0.78}Te_{0.22}$ (Ref. 6) epitaxial layers.

We have grown quaternary alloys from $(Pb_{1-x_L}Sn_{x_L})_{1-z}(Se_{1-y_L}Te_{y_L})_z$ liquid solutions with various tin contents x_L up to 20%, tellurium contents y_L of 60%, and a chalcogen content z of 3.5%. These growth solutions had liquidus temperatures in the range of 615 °C, and growth from them directly on BaF_2 has resulted in continuous epitaxial layers. We have chosen, though, to generate phase equilibria data in the 530 °C temperature range because this is the range over which active layers for DH lasers will be grown. The first layer for a DH laser structure will be a $PbSe_{0.78}Te_{0.22}$ cladding layer grown at a temperature above 610 °C. Subsequent LPE layers are then grown at lower temperatures to reduce interdiffusion of dopants across the heterojunction interfaces. As opposed to direct growth on BaF_2, $Pb_{1-x_S}Sn_{x_S}Se_{1-y_S}Te_{y_S}$ growth at 530 °C on chemically similar $PbSe_{0.78}Te_{0.22}$ is expected to yield continuous layers.

Lattice parameter mismatch between the BaF_2 substrate and the IV–VI semiconductor alloy was measured with a Rigaku x-ray diffractometer. Such analysis is possible because the quaternary IV–VI semiconductor crystallites are well-oriented with the BaF_2 substrate. Figure 3 is a typical x-ray diffraction rocking curve showing the second order (222) Cu $K\alpha_1$ and $K\alpha_2$ peaks for the (111)

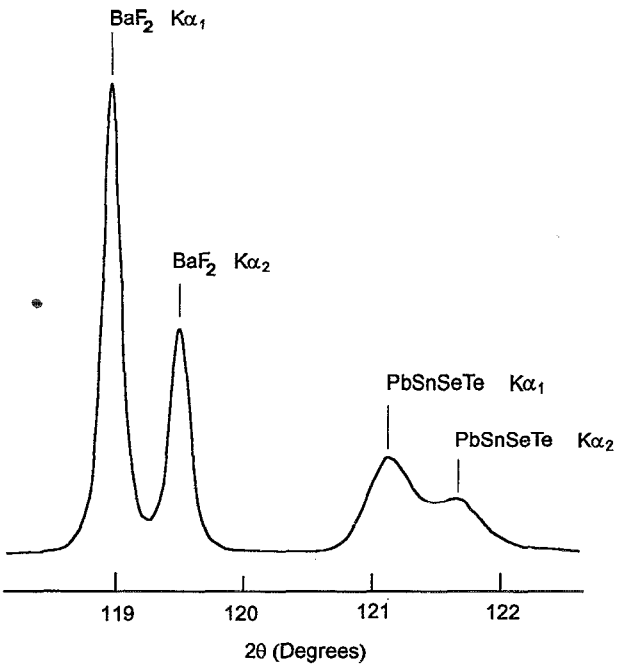

FIG. 3. Typical x-ray diffraction rocking curve for $Pb_{1-x_S}Sn_{x_S}Se_{1-y_S}Te_{y_S}$ crystallites on (111) BaF_2. The crystallites, having a little over 1% lattice mismatch with the substrate, were grown from a $(Pb_{0.40}Sn_{0.60})_{0.99}(Se_{0.65}Te_{0.35})_{0.01}$ liquid solution.

BaF_2 substrate and the IV–VI semiconductor material. The lattice parameter of the IV–VI semiconductor alloy was calculated using the 6.200 Å lattice parameter of BaF_2 as an internal standard.

The x-ray data, Eq. (1), and previously determined liquid-solid phase equilibria data for the $Pb_{1-x_S}Sn_{x_S}Se$ ternary alloys,[2] that follow the relationship

$$x_S = 1.93x_L^3 - 1.96x_L^2 + 1.03x_L, \tag{5}$$

were used to calculate the composition of the quaternary material. This method of calculating $Pb_{1-x_S}Sn_{x_S}Se_{1-y_S}Te_{y_S}$ solid composition assumes that the liquid-solid segregation coefficients for the metal (Pb and Sn) and nonmetal (Se and Te) atoms are independent. $Pb_{1-x_S}Sn_{x_S}Se_{1-y_S}Te_{y_S}$ compositions determined using Auger electron spectroscopy have agreed well with compositions calculated from x-ray data using the above assumption.[2] These data and, moreover, work by Davarshvili *et al.*[8] showing that the composition of the metal sublattice is, indeed, independent of the tellurium content in the liquid growth solution justify our assumption.

IV. RESULTS

Measured lattice parameters of the various IV–VI semiconductor alloys grown in this study are plotted as a function of tellurium content in the liquid solution y_L for three different tin contents, x_L=20%, 40%, and 60%, in Figs. 4, 5, and 6, respectively. For each tin concentration, the lattice parameter increases as the tellurium concentration increases. The lattice-matching conditions with BaF_2

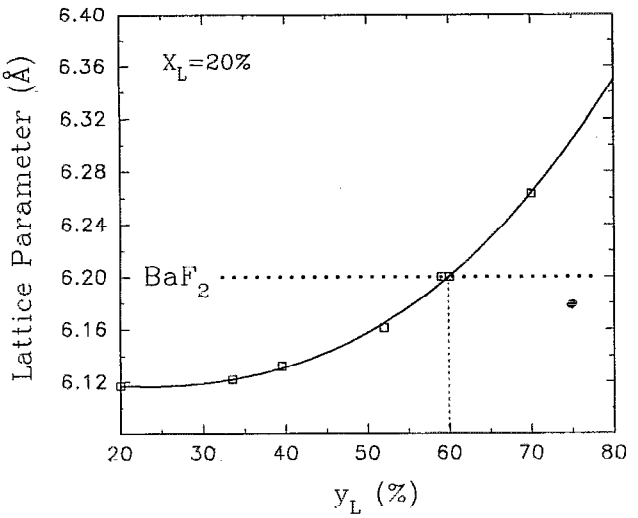

FIG. 4. Lattice parameters of $Pb_{1-x_S}Sn_{x_S}Se_{1-y_S}Te_{y_S}$ alloys grown from $(Pb_{0.80}Sn_{0.20})_{0.99}(Se_{1-y_L}Te_{y_L})_{0.01}$ liquid solutions vs tellurium content y_L. Lattice matching with BaF_2 is at $y_L=60\%$.

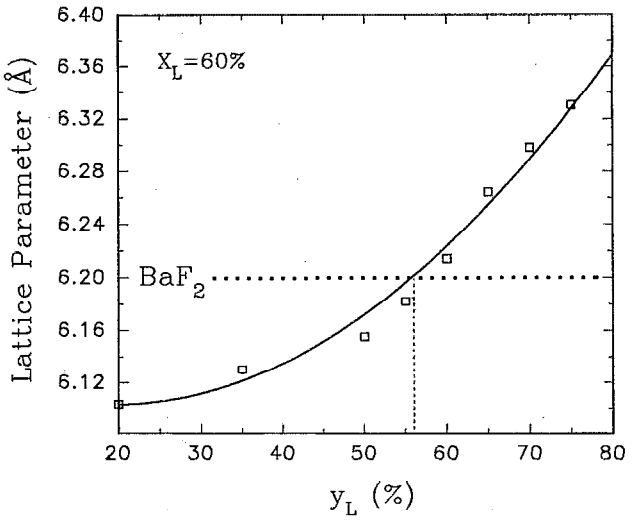

FIG. 6. Lattice parameters of $Pb_{1-x_S}Sn_{x_S}Se_{1-y_S}Te_{y_S}$ alloys grown from $(Pb_{0.40}Sn_{0.60})_{0.99}(Se_{1-y_L}Te_{y_L})_{0.01}$ liquid solutions vs tellurium content y_L. Lattice matching with BaF_2 is at $y_L=57\%$.

are $y_L=60\%$, 58%, and 57%, respectively. Table I summarizes these data along with the previously determined condition for lattice matching the ternary $PbSe_{0.78}Te_{0.22}$ alloy with BaF_2. Values for tin and tellurium content in the liquid and solid are listed along with the calculated band gap energy and cutoff wavelength at 77 K for each composition.

The fourth alloy composition listed in Table I, $Pb_{0.67}Sn_{0.33}Se_{0.65}Te_{0.35}$, is similar to the composition, $Pb_{0.70}Sn_{0.30}Se_{0.70}Te_{0.30}$, of Ref. 14 that had a measured lattice parameter of 6.195 Å. Interpolating the data in Ref. 14, the composition with the same 6.200 Å as BaF_2 is $Pb_{0.66}Sn_{0.34}Se_{0.66}Te_{0.34}$, almost identical to that listed in Table I. This is further confirmation that our procedure for calculating solid composition is accurate and that the assumption of independent liquid-to-solid segregation coefficients for metal and nonmetal atoms is valid.

The relationship between tellurium content in the solid y_S and tellurium content in the liquid y_L is shown in Fig. 7. The y_S values were calculated from the x-ray data using Eqs. (1) and (5). These data show that the liquid-to-solid segregation coefficient for tellurium is relatively small for y_L, less than 40%.

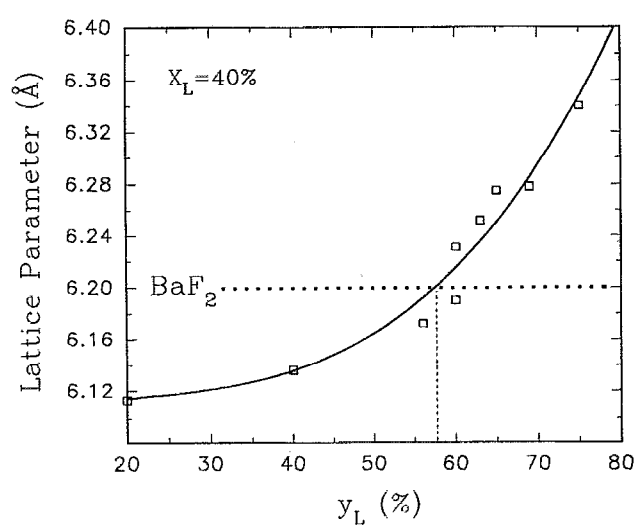

FIG. 5. Lattice parameters of $Pb_{1-x_S}Sn_{x_S}Se_{1-y_S}Te_{y_S}$ alloys grown from $(Pb_{0.60}Sn_{0.40})_{0.99}(Se_{1-y_L}Te_{y_L})_{0.01}$ liquid solutions vs tellurium content y_L. Lattice matching with BaF_2 is at $y_L=58\%$.

V. DISCUSSION

The data listed in Table I show that tellurium content in the liquid growth solution y_L decreases from 60% to 57%, while the tellurium content in the solid solution y_S actually increases from 22.2% to 34.6%. Clearly, the role of tin content in the solid, which increases with the tellurium content according to Eq. (2), needs to be considered to account for this observation.

Since LPE growth takes place under near equilibrium conditions, we can say that tellurium's chemical potential in the solid solution alloy equals its chemical potential in the liquid growth solution,

$$\mu_{\mathrm{Te}}^{S}=\mu_{\mathrm{Te}}^{L}. \tag{6}$$

TABLE I. Compositions of liquid $(Pb_{1-x_L}Sn_{x_L})_{0.99}(Se_{1y_L}Te_{y_L})_{0.01}$ solutions that yield $Pb_{1-x_S}Sn_{x_S}Se_{1-y_S}Te_{y_S}$ alloys lattice matched with BaF_2. Corresponding band gap energies and cutoff wavelengths at 77 K are also listed.

x_L (%)	y_L (%)	x_S (%)	y_S (%)	E_g (meV)	λ (μm)
0	60	0	22.2	185	6.72
20	60	14.3	27.5	73.5	16.9
40	58	22.2	30.5	14.2	87.5
60	57	32.9	34.6	−63.5	19.6

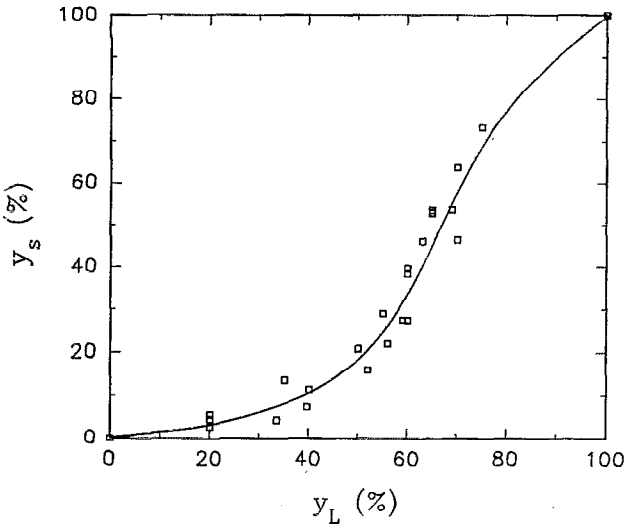

FIG. 7. Composition of group VI sublattice y_S vs tellurium content in liquid growth solution y_L. A small, relative to selenium, liquid-to-solid segregation coefficient for tellurium is apparent for y_L, less than 40%.

If we assume that tellurium behaves ideally in the liquid growth solution, then the chemical potential of tellurium in the solid can be expressed as

$$\mu_{\mathrm{Te}}^{S}=\mu_{\mathrm{Te}}^{L,o}+\mathrm{RT}\ln y_L. \tag{7}$$

Equation (7) shows that the tellurium chemical potential in $Pb_{1-x_S}Sn_{x_S}Se_{1-y_S}Te_{y_S}$ solid solutions decreases as the tellurium concentration in the liquid growth solution decreases. Since y_S increases as y_L decreases for $Pb_{1-x_S}Sn_{x_S}Se_{1-y_S}Te_{y_S}$ alloys lattice matched with BaF_2, we have a situation in which the chemical potential of tellurium actually decreases as its concentration in the solid increases.

Possible explanations for the highly nonideal behavior of $Pb_{1-x_S}Sn_{x_S}Se_{1-y_S}Te_{y_S}$ solid solutions involve chemical bond energy and/or atomic size differences. Table II lists enthalpies of formation for PbSe, PbTe, SnSe, and SnTe. The selenides have higher bond energies than the tellurides, while the lead compounds have higher bond energies than the tin compounds. Table III lists ionic radii for Pb, Sn, Se, and Te atoms showing that tellurium is larger than selenium, while tin is smaller than lead, size differences that are reflected in the lattice parameters of the binary compounds.

TABLE II. Enthalpy of formation at 298 K for binary IV–VI compounds.

Alloy	ΔH_{fus}, 298 K	(kJ/mol)
PbSe	−99.6[a]	...
PbTe	−69.1[a]	−68.5[b]
SnSe	−88.7[a]	...
SnTe	−60.7[a]	−58.7[c]

[a]See Ref. 18.
[b]See Ref. 19.
[c]See Ref. 20.

TABLE III. Ionic radii of group IV and group VI elements.[a]

Element	Valence	Radius (Å)
Pb	+2	1.20
Sn	+2	0.93
Se	−2	1.91
Te	−2	2.11

[a]See Ref. 18.

Figure 7 shows that $Pb_{1-x_S}Sn_{x_S}Se_{1-y_S}Te_{y_S}$ solid solutions that have small tellurium concentrations are in equilibrium with liquid solutions that have relatively large tellurium concentrations. These alloys thus have relatively large tellurium chemical potentials according to Eq. (7). Both bond energy and atomic size effects can account for a high tellurium chemical potential in $Pb_{1-x_S}Sn_{x_S}Se_{1-y_S}Te_{y_S}$ solid solutions. Tellurium, having lower bond energies than selenium with lead and tin, will have a smaller affinity to the solid. Also, the incorporation of large (relative to selenium) tellurium atoms in the growing solid can cost energy in the form of lattice strain. Relaxation of this lattice strain can, therefore, be a driving force for high tellurium chemical potential.

In the quaternary solid, tin atoms replace lead atoms on the group IV sublattice, thus changing the chemical environment for tellurium in the solid. Since tellurium is less strongly bound to tin than it is to lead, addition of tin would reduce the affinity that tellurium has for the $Pb_{1-x_S}Sn_{x_S}Se_{1-y_S}Te_{y_S}$ solid. In other words, if chemical effects alone were considered, an increasing tin concentration would increase the tellurium chemical potential. This is opposite of what is observed, suggesting that bond energy difference is not the dominant factor in determining tellurium chemical potential in $Pb_{1-x_S}Sn_{x_S}Se_{1-y_S}Te_{y_S}$ solid solutions.

Substitution of lead atoms with relatively small tin atoms in the quaternary alloy creates more space on the group VI sublattice to accommodate relatively large tellurium atoms. Increasing the tin concentration in the quaternary alloy can thus reduce the amount of strain energy associated with the incorporation of tellurium into the growing solid. Reduction of this strain energy will tend to increase the affinity that tellurium has for the $Pb_{1-x_S}Sn_{x_S}Se_{1-y_S}Te_{y_S}$ solid. This is consistent with what is observed in that less tellurium is required in the liquid solution to achieve lattice matching, i.e., higher tellurium content in the solid, as the tin concentration is increased. We therefore conclude that composition dependent lattice strain is the dominant factor in determining tellurium chemical potential in $Pb_{1-x_S}Sn_{x_S}Se_{1-y_S}Te_{y_S}$ quaternary alloys that are lattice matched with BaF_2.

VI. SUMMARY

A series of $Pb_{1-x_S}Sn_{x_S}Se_{1-y_S}Te_{y_S}$ solid solution IV–VI semiconductor alloys have been grown on BaF_2 substrates by liquid phase epitaxy. Liquid-solid phase equilibria data

show that, although tellurium content in the solid increases as the tin content increases, tellurium concentration in the $(Pb_{1-x_L}Sn_{x_L})_{0.99}(Se_{1-y_L}Te_{y_L})_{0.01}$ liquid growth solution actually decreases slightly. A model has been proposed that explains this behavior in terms composition dependent lattice strain: an increasing tin concentration on the metal sublattice can reduce the lattice strain associated with tellurium incorporation, thus reducing a relatively large tellurium chemical potential in these alloys. These data can be used for LPE growth of lattice-matched IV–VI semiconductor heterostructures on BaF_2 substrates. Such growth will facilitate development of novel far-infrared tunable diode lasers.

ACKNOWLEDGMENTS

This work was supported by grants from the Oklahoma Center for Advancement of Science and Technology and the National Science Foundation.

[1] Y. Horikoshi, M. Kawashima, and H. Saito, Jpn. J. Appl. Phys. **21**, 77 (1982).
[2] P. J. McCann, J. Fuchs, Z. Feit, and C. G. Fonstad, J. Appl. Phys. **62**, 2994 (1987).
[3] H. Holloway, E. M. Logothesis, and E. Wilkes, J. Appl. Phys. **41**, 3543 (1970).
[4] H. Zogg, S. Blunier, and J. Masek, J. Electrochem. Soc. **136**, 775 (1989).
[5] H. Zogg, J. Masek, C. Maissen, S. Blunier, and H. Weibel, Thin Solid Films **184**, 247 (1990).
[6] P. J. McCann and C. G. Fonstad, Thin Solid Films **227**, 185 (1993).
[7] D. Kasemset, S. Rotter, and C. G. Fonstad, J. Electron. Mater. **10**, 863 (1981).
[8] O. I. Davarshvili, V. P. Zlomanov, I. V. Krialashvili, M. I. Saginuri, R. I. Chikovani, and A. P. Shotov, Sov. Phys. Dokl. **28**, 885 (1983).
[9] J. N. Walpole, A. R. Calawa, T. C. Harman, and S. H. Groves, Appl. Phys. Lett. **28**, 552 (1976).
[10] A. J. Strauss, Phys. Rev. **157**, 608 (1967).
[11] J. O. Dimmock, I. Melngailis, and A. J. Strauss, Phys. Rev. Lett. **16**, 1193 (1966).
[12] H. Krebs, K. Grun, and D. Kallen, Z. Anorg. Allg. Chem. **312**, 307 (1961).
[13] B. A. Volkov, O. A. Pankratov, and A. V. Sazonov, Sov. Phys. Solid State **26**, 255 (1984).
[14] P. M. Nikolic, Brit. J. Appl. Phys. **18**, 897 (1967).
[15] P. J. McCann and C. G. Fonstad, J. Cryst. Growth **114**, 687 (1991).
[16] P. J. McCann and C. G. Fonstad, J. Electron. Mater. **20**, 915 (1991).
[17] P. J. McCann, Mater. Res. Soc. Symp. Proc. **221**, 289 (1991).
[18] *Handbook of Chemistry and Physics,* 48th ed., edited by R. C. Weast (The Chemical Rubber Company, Cleveland, OH, 1967).
[19] Y. Huang and R. F. Brebrick, J. Electrochem. Soc. **135**, 486 (1988).
[20] Y. Huang and R. F. Brebrick, J. Electrochem. Soc. **135**, 1547 (1988).